Optical Engineering

OpticalEngineering.SPIEDigitalLibrary.org

Generation of an ultraflat and power efficient optical frequency comb by cascading of electroabsorption and single-drive Mach–Zehnder modulator

Ujjwal
Jaisingh Thangaraj

SPIE.

Ujjwal, Jaisingh Thangaraj, "Generation of an ultraflat and power efficient optical frequency comb by cascading of electroabsorption and single-drive Mach–Zehnder modulator," *Opt. Eng.* **57**(12), 126106 (2018), doi: 10.1117/1.OE.57.12.126106.

Downloaded From: https://www.spiedigitallibrary.org/journals/Optical-Engineering on 1/3/2019
Terms of Use: https://www.spiedigitallibrary.org/terms-of-use

Generation of an ultraflat and power efficient optical frequency comb by cascading of electroabsorption and single-drive Mach–Zehnder modulator

Ujjwal* **and Jaisingh Thangaraj**
Indian Institute of Technology (Indian School of Mines), Department of Electronics Engineering Dhanbad, India

Abstract. We have investigated the theoretical and principal analysis of cascaded electroabsorption modulators (EAMs) and Mach–Zehnder modulator (MZM). We have proposed a technique to generate an ultraflat and power efficient optical frequency comb (OFC) by the serial cascading of two EAMs and one single-drive MZM. Continuous wave (CW) light source is modulated and spectrum broadened by two EAMs and MZM, respectively. Here, EAMs in cascaded mode produce ultrashort pulses followed by MZM, which is introduced to perform intensity modulation and tuned the power variation of even and odd order sidebands at the same level for obtaining a flat optical spectrum at the output. The first EAM acts as a subcarrier generator and the latter one acts as a subcarrier enhancer, which is followed by the MZM acting as subcarrier flatter. By this proposed technique, we have generated 63 subcarriers with 10-GHz spacing and within 2-dB power fluctuation. The generated OFC has a bandwidth of 630 GHz. This technique generates OFC with an appreciable power level and flattened optical spectrum, which is very much essential in dense wavelength division multiplexing and elastic optical networks. © *2018 Society of Photo-Optical Instrumentation Engineers (SPIE)* [DOI: 10.1117/1.OE.57.12.126106]

Keywords: electroabsorption modulator; optical frequency comb; Mach–Zehnder modulators.

Paper 181077 received Jul. 27, 2018; accepted for publication Nov. 28, 2018; published online Dec. 18, 2018.

1 Introduction

In recent days, optical frequency combs (OFCs) are mostly preferred for measuring frequency due to their outstanding accuracy, large spectral coverage, and high-spectral purity. OFCs are initially developed to establish a link between the optical and radio frequency domain. Now, it is used in many fields such as dense wavelength division multiplexing,[1] arbitrary waveform generation,[2] optical signal processing,[3] RF photonics,[4] optical communications,[5] and optical code division multiple access.[6] There are many methods for generating OFC that include mode-locked laser, which provides a large number of subcarriers with high repetition rate. The disadvantages in this technique are cavity complexity and carrier-envelope offset stabilization.[7] Alternatively, generation of OFC by cascading of electro-optical modulators, such as phase modulator (PM) and intensity modulators (IMs), have been proved to be very efficient and cost-effective. These methods have many advantages such as alterable wavelength, intelligible configuration, and independently adjusting the comb lines spacing. An electro-optic modulator generates a train of sidebands when driven by an RF sinusoidal signal. These sidebands can be considered as OFC. Thus, for the generation of a large number of sidebands or comb lines, more modulators are required. There are many configurations, and setups consisting of different electro-optic modulators have been presented. Cascading of two IM generates nine comb lines within 2-dB power fluctuations, and it generates 38-comb lines within 2-dB power fluctuations when it is driven by the tailored RF clock.[8] By driving the Mach–Zehnder modulator (MZM) with first- and second-order harmonics of the RF sinusoidal signal, 11-subcarriers with less than 1-dB power deviation are generated.[9] In Ref. 10, 29 comb lines are generated within 1.5-dB power fluctuations through cascading of one IM and two PM. Cascading of IM and PM generates 15 comb lines within 1-dB power fluctuation.[11] From the above-discussed techniques, it is found that an OFC generated by the cascading of EAMs and single-drive MZM produces a larger number of subcarriers with a good power level and spectral flatness

In this paper, we have proposed an ultraflat and wideband generation of OFC by serially cascading of two electroabsorption modulators (EAM) followed by one single-drive MZM. All these modulators are driven by sinusoidal RF signal at frequency f_r, $f_r/2$, and f_r, respectively. The applied sinusoidal voltage drive gets converted into ultrashort optical pulses due to the nonlinear transfer function of the EAM, and it is further compressed by another cascaded EAM. These ultrashort pulses in the frequency domain are called OFC. But the comb lines at the output of EAM has power variation around 40 dB resulting in poor spectral flatness. Therefore, to obtain a flat spectrum, the EAM output is fed into MZM, which performs the amplitude gating of the optical spectrum and energized the weak sidebands to get a flattened spectrum at the output. Hence, the generated OFC offers a flat power spectrum with high stability and less complexity. We have obtained 63 subcarriers with 10-GHz spacing and within 2-dB spectral ripple fluctuation. From our proposed technique, we have generated the OFC with a bandwidth of 630 GHz. We have also performed the theoretical analysis of cascading EAMs and MZM. The rest of the paper is organized as follows: Sec. 2 explains the principle of operation followed by the theoretical analysis and discussion in Sec. 3 and concluded in Sec. 4.

*Address all correspondence to Ujjwal, E-mail: yadavujjwal1992@gmail.com

0091-3286/2018/$25.00 © 2018 SPIE

Downloaded From: https://www.spiedigitallibrary.org/journals/Optical-Engineering on 1/3/2019
Terms of Use: https://www.spiedigitallibrary.org/terms-of-use

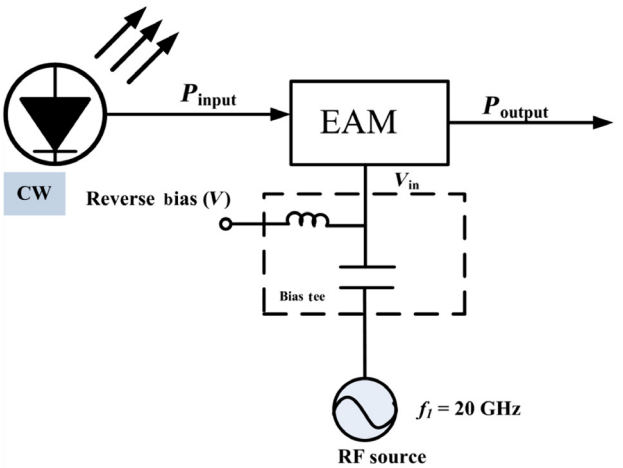

Fig. 1 Single EAM-based optical short-pulse generator.

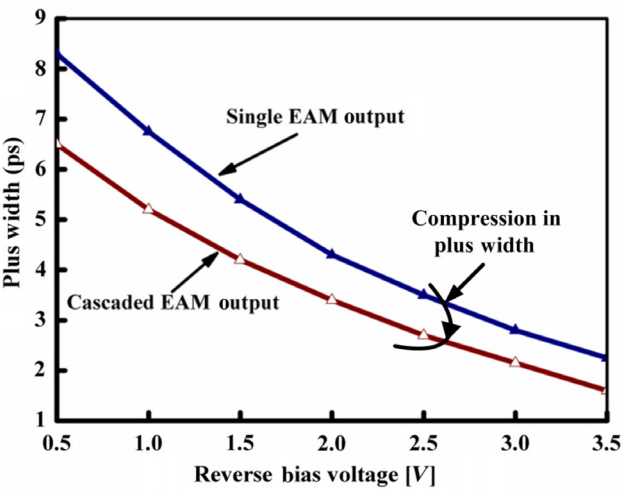

Fig. 3 The variation in pulse width (FWHM) with respect to the reverse bias voltage.

2 Principle of Operation

In our proposed technique, we have generated the OFC by connecting EAM and MZM in cascaded mode. EAM is a semiconductor device that modulates the intensity of light via an electric field. Its operating principle is based on the Franz–Keldysh effect. It is the change in the absorption spectrum due to applied electric field, which alters the energy gap. It does not involve the carrier excitation due to electric field. EAM provides many benefits in comparison to electro-optic modulators such as small size, low driving voltage, less sensitive to polarization, high modulation bandwidth, ultrahigh speed modulation, large footprint, and ability to integrate with optoelectronic devices.[12] EAM is mostly preferred for the generation of short optical pulses due to its nonlinear optical absorption characteristic (shown in Fig. 1).

Here, continuous wave light generated by single-mode laser is fed into EAM. On applying a reverse biased sinusoidal signal at the electrical input, CW light is converted into short pulses. These ultrashort pulses are referred to as OFC in the frequency domain. The absorption of EAM can be represented as a function of input electrical voltage (V_{in}) as EAM (V_{in}). It is the extinction ratio of the optical output (P_{output}) with respect to the optical input (P_{input}):

$$\mathrm{Ext\,(dB)} = P_{output}\,(\mathrm{dBm}) - P_{input}\,(\mathrm{dBm}) = \mathrm{EAM}(V_{in}), \quad (1)$$

$$P_{output}\,(\mathrm{dBm}) = P_{input}\,(\mathrm{dBm}) + \mathrm{Ext\,(dB)}. \quad (2)$$

The variation in the full-width half-maximum (FWHM) of the generated pulses with respect to the reverse bias voltage at the output of single EAM is shown in Fig. 3. The bias voltage is changed from 0.5 to 3.5 V in the steps of 0.5 V and pulses are examined at RF drive voltage of 3.7 Vpp. For achieving higher extinction ratio and further compression in the pulse width (FWHM), two EAMs are connected in cascaded mode as shown in Fig. 2.

In this arrangement, signal is handled by two cascaded EAMs. Here, we conceive the optical output (P_{output}) as the initial optical input to the previous EAM. In other term, it can be obtained by subsequently changing the extinction from the first and the latter EAM:

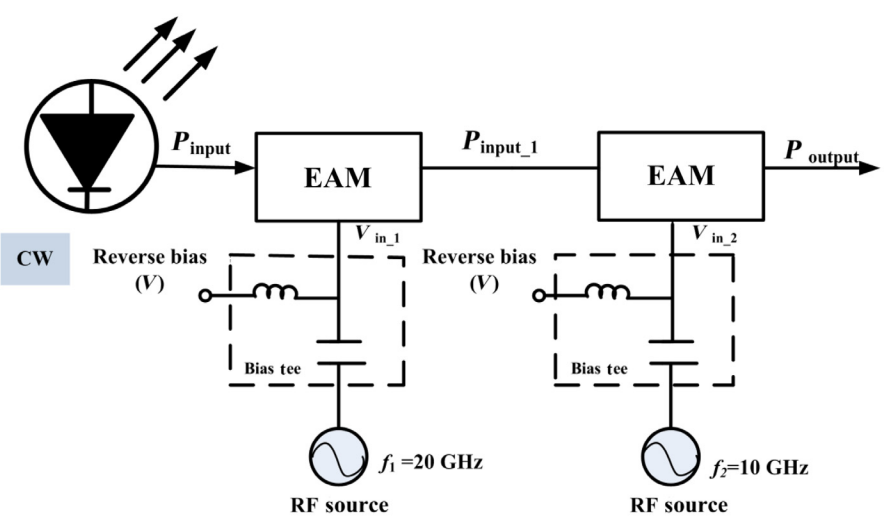

Fig. 2 Cascaded EAM-based optical short-pulse generator.

Downloaded From: https://www.spiedigitallibrary.org/journals/Optical-Engineering on 1/3/2019
Terms of Use: https://www.spiedigitallibrary.org/terms-of-use

$$P_{\text{output}} = P_{\text{input\_1}} + \text{EAM}(V_{\text{in\_2}}), \tag{3}$$

$$P_{\text{input\_1}} = P_{\text{input}} + \text{EAM}(V_{\text{in\_1}}). \tag{4}$$

Substituting Eq. (4) into Eq. (3), we obtain

$$P_{\text{output}} = P_{\text{input}} + \text{EAM}(V_{\text{in\_1}}) + \text{EAM}(V_{\text{in\_2}}). \tag{5}$$

We can rewrite the P_{output} considering the optical extinction where EAM $(V_{\text{in\_1}}) = \text{Ext}_1(t)$ and EAM $(V_{\text{in\_2}}) = \text{Ext}_2(t)$:

$$P_{\text{output}} = P_{\text{input}} + \text{Ext}_1(t) + \text{Ext}_2(t). \tag{6}$$

Cascaded EAMs structure mentioned earlier results in high pulse extinction ratio. The variation in FWHM of the generated pulses with respect to the reverse bias voltage at the output of cascaded EAMs is shown in Fig. 3.

Considering the above results, we found that cascading of two EAMs results in a significant improvement in the extinction ratio and compression in the pulse width (FWHM) around 30% thereby broadening the optical spectrum in frequency domain but with poor spectral flatness. Therefore, in order to achieve flattened spectrum, EAMs are cascaded with MZM. MZM is an external electro-optic modulator which performs optical intensity modulation using electro-optic effect. It can be of either single drive or dual drive. Single-drive MZM has a very simple configuration and can work at the high modulation frequency. In our proposed model, we use single-drive MZM for intensity modulation. The basic structure of single-drive MZM is shown in Fig. 4.

It comprises of two waveguides that form the arms of interferometer. Each interferometer arm is surrounded by electrodes. These electrodes are connected to the bias voltage and RF voltage to alter the phase in both the arms. On coupling the optical spectrum at the output of EAM with MZM (input waveguide) where the spectrum gets split equally into interferometer arms. On applying the electric voltages, the refractive index of each interferometer arm changes according to electro-optic effect. This change in refractive index causes phase modulation of the optical spectrum that is propagating through the arms of MZM according to the applied voltages. By combining the two arms of the

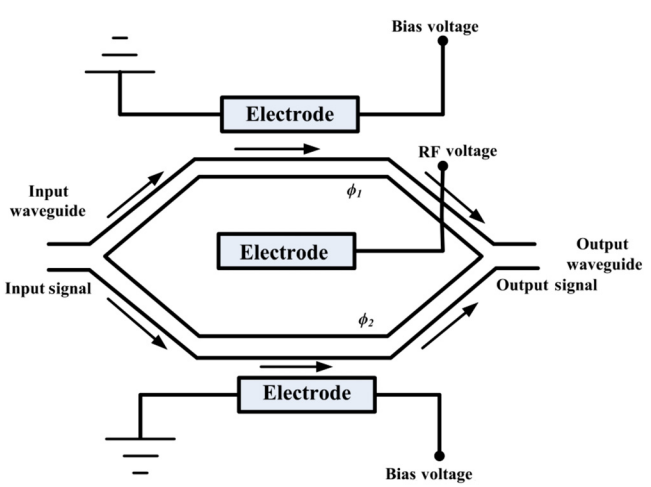

Fig. 4 Single-drive MZM.

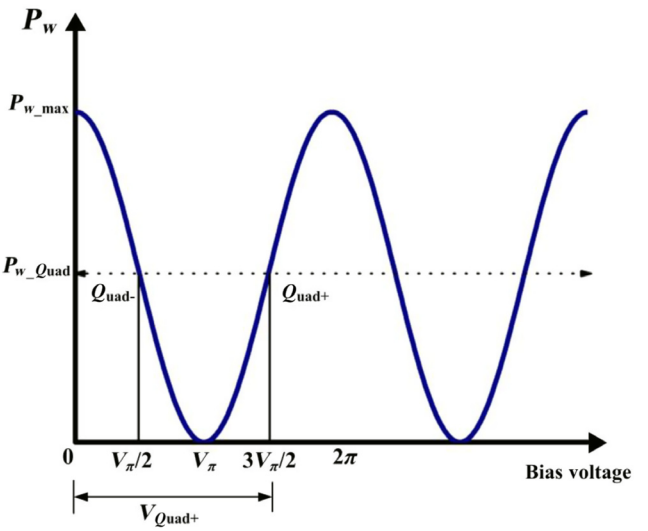

Fig. 5 Transfer characteristics of the MZM.

interferometer, phase modulation is converted into intensity modulation.[13–15] This makes the MZM to function as an IM. This IM performs the amplitude gating of the optical spectrum and energized the weak sidebands to get a flattened spectrum at the output. For the proper functioning of MZM, it is essential to understand the effect of DC bias voltage on the output signal. DC bias voltage is the main controlling factor for setting a desired operating point for any specific application.

In our proposed work, DC bias voltage ($V_{\text{Quad+}} = 3V_\pi/2$, V_π is the half-wave voltage) is applied to the MZM for the setting of positive slop quadrature point Quad+ (desired operating point). At the positive slop quadrature point Quad+, it starts to function as an IM which generates a flattened spectrum at the output. The transfer function between output optical power (P_w) and DC bias voltage is shown in Fig. 5.

Figure 6 shows the principle of generation of OFC by the serially cascading of two EAM and one MZM. Here, laser diode is connected in the cascaded mode with two EAM and one MZM for the generation of OFC. They are driven by sinusoidal RF signal at frequency f_r, $f_r/2$, and f_r, respectively. These modulators are directly driven by RF signals without using amplifier and phase shifter, which makes this approach worthwhile. The first EAM acts as subcarrier generator, the latter EAM acts as subcarrier enhancer, and MZM acts as subcarrier flatter.

The specification of all the devices along these lines include: a 1550-nm laser with output power of 10 mW and a linewidth of 1 MHz, reversed bias voltage (V) and RF drive voltage (V_{RF}) of EAMs are 3.2 V and 3.7 Vpp, respectively. The bias voltage ($V_{\text{Quad+}}$) of MZM is 7 V, half-wave voltage (V_π) is 4.5 V, the extinction ratio is 30 to 35 dB and symmetry factor is 0.966. EAM1, EAM2, and MZM are driven by sinusoidal RF clocks with the frequency of 20, 10, and 20 GHz, respectively. The spectral bandwidth of the generated OFC is 630 GHz.

3 Theoretical Analysis and Discussion

In order to confirm the feasibility and necessity of the proposed OFC, we performed the theoretical and principal

Downloaded From: https://www.spiedigitallibrary.org/journals/Optical-Engineering on 1/3/2019
Terms of Use: https://www.spiedigitallibrary.org/terms-of-use

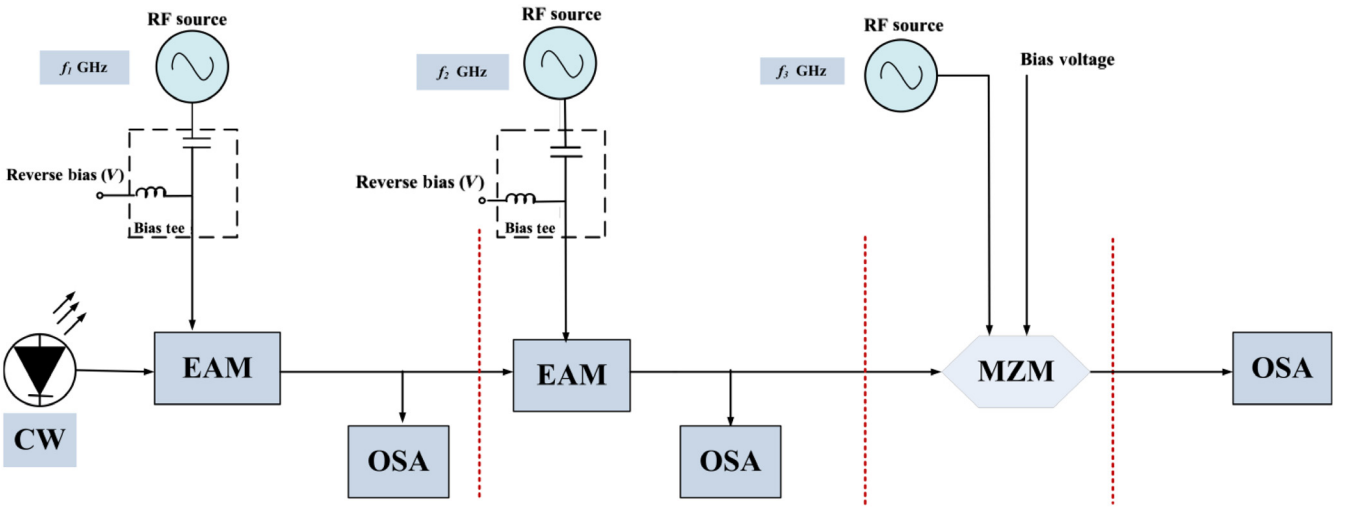

Fig. 6 Principle of OFC generation. CW, laser; EAM, electroabsorption modulator; MZM, Mach–Zehnder modulator.

analysis for the cascaded EAMs and MZM. Here, we considered for two cases: (i) driving the cascaded EAMs and MZM by sinusoidal RF signal at frequency ($f_1 = f_r$ GHz, $f_2 = f_r/2$ GHz and $f_3 = f_r$ GHz (proposed OFC generation technique), (ii) driving all the modulators by the same RF sinusoidal signal at frequency ($f_1 = f_2 = f_3 = f_r$ GHz). The transfer function of EAM is mentioned in Eq. (7) as in Ref. 16:

$$T(V) = \frac{P_{\text{out}}}{P_{\text{in}}} = \exp[-\Gamma_\alpha(V)L], \tag{7}$$

where P_{in} and P_{out} are the input and output power of the laser, Γ represents the confinement factor, α represents the absorption coefficient, and L represents the length of the EAM. On considering the dc biased voltage and modulating voltage of EAM to be V_d and V_m, the net voltage is $V = V_d + V_m$:

$$V = V_d(1 + m_0 \cos w_m t), \tag{8}$$

$$V_m = ([V_d m_0 \cos(w_m)t)], \tag{9}$$

where m_0 is the modulation index and $\cos(w_m)$ is the driving signal of EAM. Transfer function of EAM is nonlinear. Due to its nonlinearity property, it generates high frequency harmonics. The spectral bandwidth of EAM is calculated by expanding the transfer function using Taylor series at dc bias V_d:

$$T(V) = T(V_d) + (V - V_d)T^{(1)}(V_d) + \frac{1}{2!}(V - V_d)^2 T^{(2)}(V_d) + \frac{1}{3!}(V - V_d)^3 T^{(3)}(V_d) + \ldots, \tag{10}$$

$$V - V_d = B_m \cos w_m t. \tag{11}$$

The transfer function of the first EAM driven by a sinusoidal RF signal at f_1 can be represented as mentioned in Eqs. (12) and (13):

$$T(v_1) = \left[T(v_d) + (B_m \cos 2\pi f_1 t)T^{(1)}(V_d) + \frac{1}{2!}(B_m \cos 2\pi f_1 t)^2 T^{(2)}(V_d) + \frac{1}{3!}(B_m \cos 2\pi f_1 t)^3 T^{(3)}(V_d) + \ldots\right], \tag{12}$$

$$T(v_1) = \left[T(v_d) + \sum_{n=1}^{k} \frac{1}{n!}(B_m \cos 2\pi f_1 t)^n T^{(n)}(V_d)\right]. \tag{13}$$

Nonlinear characteristics of the transfer function convert the applied RF sinusoidal modulation voltage into ultrashort pulses, which are referred to as OFC in the frequency domain. Figure 7 shows the optical spectrum at the output of first EAM driven by a sinusoidal RF signal at frequency ($f_1 = f_r = 20$ GHz).

The transfer function of the second EAM driven by a sinusoidal RF signal at f_2 is represented as mentioned in Eqs. (14) and (15):

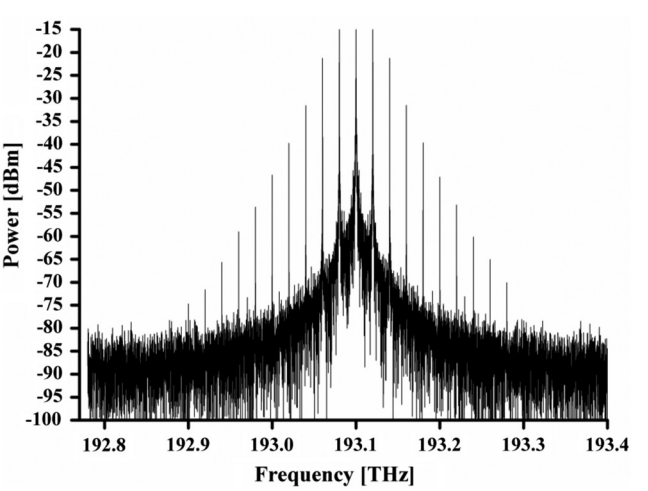

Fig. 7 Optical spectrum at the output of first EAM.

Downloaded From: https://www.spiedigitallibrary.org/journals/Optical-Engineering on 1/3/2019
Terms of Use: https://www.spiedigitallibrary.org/terms-of-use

$$T(v_2) = \left[T(V_d) + (B_m \cos 2\pi f_2 t)T^{(1)}(V_d) + \frac{1}{2!}(B_m \cos 2\pi f_2 t)^2 T^{(2)}(V_d) + \frac{1}{3!}(B_m \cos 2\pi f_2 t)^3 T^{(3)}(V_d) + \ldots\right], \quad (14)$$

$$T(v_2) = \left[T(v_d) + \sum_{n=1}^{k} \frac{1}{n!}(B_m \cos 2\pi f_2 t)^n T^{(n)}(V_d)\right]. \quad (15)$$

Cascading of two EAM compresses the ultrashort pulses thereby increasing the pulse extinction ratio. This leads to broadening of the spectrum in the frequency domain. The net transfer function at the output of serially cascaded two EAMs is given as

$$T(v_e) = T(v_1) \times T(v_2), \quad (16)$$

$$T(v_e) = [T(v_d)]^2 + \sum_{n=1}^{k} (B_m)^n T^{(n)}(v_d) \times \left[\frac{1}{n!}(\cos 2\pi f_2 t)^n T(v_d) + \frac{1}{n!}(\cos 2\pi f_1 t)^n T(v_d) + \frac{1}{2n!}(B_m)^n [\cos(f_1 + f_2)t + \cos(f_1 - f_2)t]^n T^{(n)}(v_d)\right] \quad (17)$$

The optical spectrum at the output of second EAM driven by a sinusoidal RF signal at frequency ($f_2 = f_r/2 =$ 10 GHz) and is shown in Fig. 8.

The optical spectrum at the output of second EAM driven by an RF sinusoidal signal at frequency ($f_2 = f_r =$ 20 GHz) and is shown in Fig. 9.

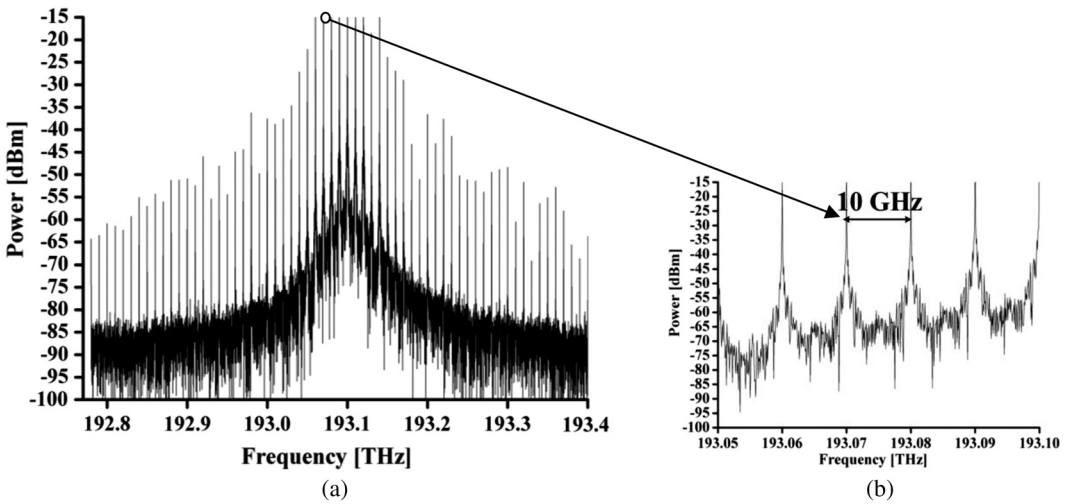

Fig. 8 (a) Optical spectrum at the output of the second EAM driven by ($f_2 = f_r/2 = 10$ GHz) RF sinusoidal signal and (b) frequency spacing between comb lines.

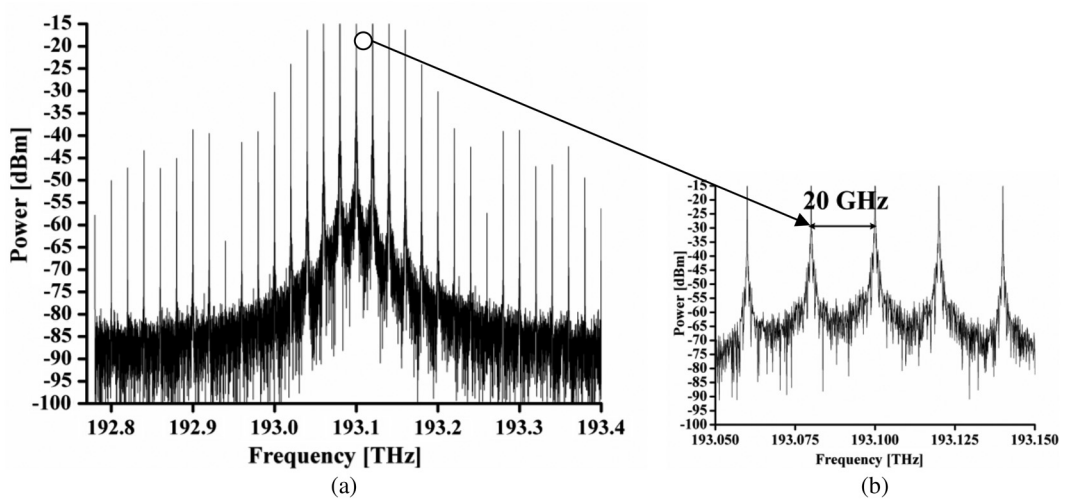

Fig. 9 (a) Optical spectrum at the output of the second EAM driven by ($f_2 = f_r = 20$ GHz) RF sinusoidal signal and (b) frequency spacing between comb lines.

Downloaded From: https://www.spiedigitallibrary.org/journals/Optical-Engineering on 1/3/2019
Terms of Use: https://www.spiedigitallibrary.org/terms-of-use

When the latter EAM is driven by a sinusoidal RF signal at frequency ($f_2 = f_r/2$ GHz), it functions as subcarrier enhancer and increases the pulse repetition rate which produces number of subcarriers as shown in Fig. 8. However, it inhibits the generation of subcarriers while driven by same sinusoidal RF signal ($f_2 = f_r$ GHz) due to the cancellation of spectral components as shown in Eq. (17).

Optical spectrum at the output of second EAM has poor spectral flatness. Next, the generated comb lines are fed into MZM which performs amplitude gating and energized the weak sidebands resulting in a flattened optical spectrum.

When an optical source at frequency f_0 is modulated by an MZM which is driven by an RF sinusoidal signal at frequency f_3, the net electric field that is available at the output of two arms is

$$E(t) = E_1(t) + E_2(t). \tag{18}$$

$$E(t) = \frac{1}{2}E_0[e^{j(2\pi f_0 t+\beta_1 v(t)+\varnothing_{01})} + e^{j(2\pi f_0 t+\beta_2 v(t)+\varnothing_{02})}]. \tag{19}$$

The static phase of each arm is Φ_{01} and Φ_{02}, respectively, β_1 and β_2 denote the voltage to phase conversion coefficient of the arms of the MZM modulator. If the applied RF sinusoidal modulation voltage is $v(t) = V_m \sin 2\pi f_3 t$ then net electric field can be expressed as

$$E(t) = \frac{1}{2}E_0 e^{jn2\pi f_0 t}[e^{j(\beta_1 v_m \sin 2\pi f_3 t+\varnothing_{01})} + e^{j(\beta_2 v_m \sin 2\pi f_3 t+\varnothing_{02})}]. \tag{20}$$

Using Bessel series expansion, we analyzed the complete harmonic components at the output of MZM. The transfer function of the MZM can be represented as

$$T(v_3) = \left[\frac{1}{2}\sum_{n=-\infty}^{\infty} j_n(b_1)e^{j\varnothing_{01}} + j_n(b_2)e^{j\varnothing_{02}}\right]e^{jn2\pi f_3 t}, \tag{21}$$

where $b_{1,2} = v_m\beta_{1,2}$.

Optical spectrum at the output of second EAM ranges from $n = 1$ to k, which is coupled into MZM. Hence $T(v_3)$ is expressed as

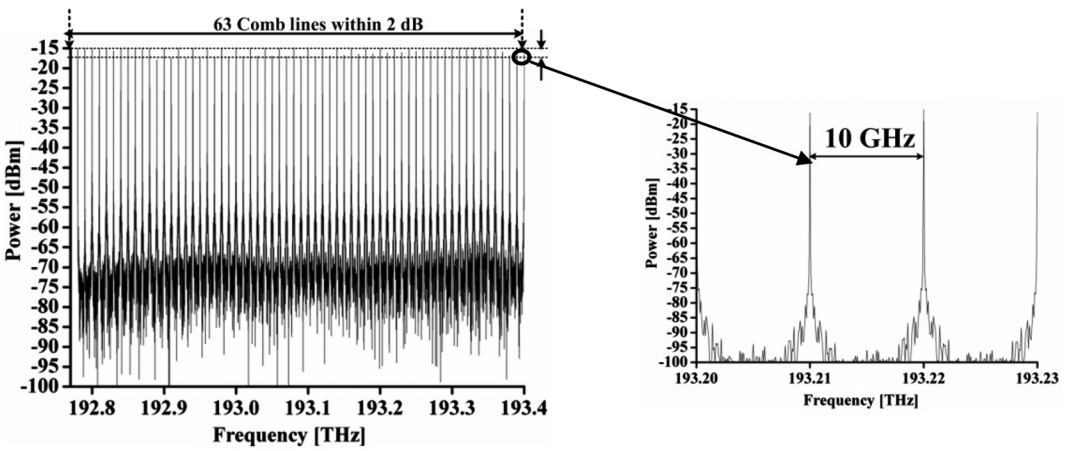

Fig. 10 (a) Optical spectrum at the output of MZM driven by ($f_3 = f_r = 20$ GHz) RF sinusoidal signal and (b) frequency spacing between comb lines (proposed OFC generation technique).

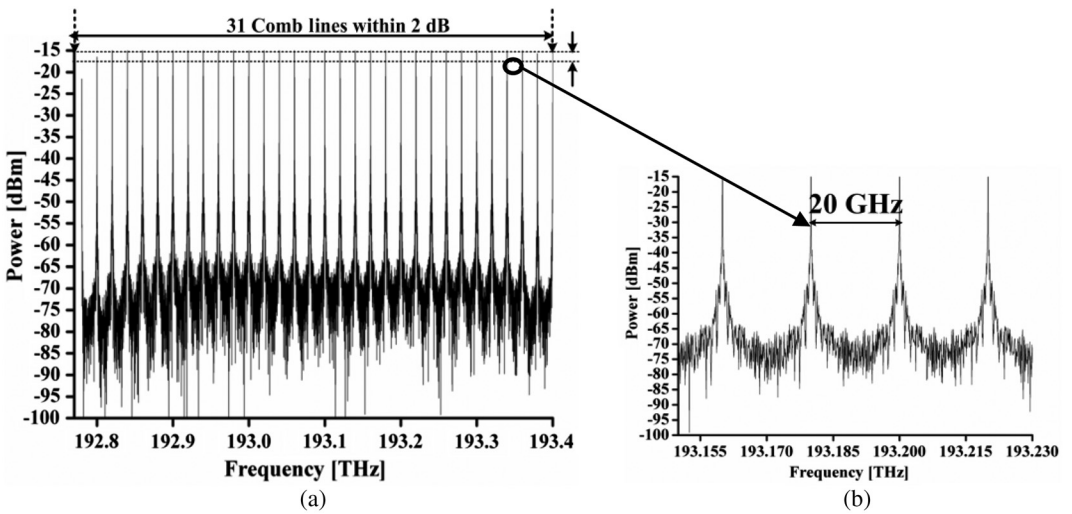

Fig. 11 (a) Optical spectrum at the output of MZM driven by ($f_1 = f_2 = f_3 = f_r = 20$ GHz) RF sinusoidal signal and (b) frequency spacing between comb lines.

Downloaded From: https://www.spiedigitallibrary.org/journals/Optical-Engineering on 1/3/2019
Terms of Use: https://www.spiedigitallibrary.org/terms-of-use

$$T(v_3) = \sum_{n=-\infty}^{0} 0 + \left[\frac{1}{2}\sum_{n=1}^{\infty} j_n(b_1)e^{j\varnothing_{01}} + j_n(b_2)e^{j\varnothing_{02}}\right]e^{jn2\pi f_3 t} + \sum_{n=k}^{0} 0, \tag{22}$$

where j_n is the first kind of Bessel function of order n.

Therefore, the overall transfer function of serially cascaded EAMs and MZM is

$$T(v) = T(v_1) \times T(v_2) \times T(v_3), \tag{23}$$

where $X_n = j_n(b_1)e^{j\varnothing_{01}} + j_n(b_2)e^{j\varnothing_{02}}$.

$$\frac{1}{2}\sum_{n=1}^{k} X_n\, e^{j2\pi n f_3 t}\left[[T(v_d)]^2 + (B_m)^n T^{(n)}(v_d) \times \left\{\frac{1}{n!}(\cos 2\pi f_2 t)^n T(v_d) + \frac{1}{n!}(\cos 2\pi f_1 t)^n T(v_d) + \frac{1}{2n!}(B_m)^n[\cos(f_1+f_2)t + \cos(f_1-f_2)t]^n T^{(n)}(v_d)\right\}\right]. \tag{24}$$

Figure 10 shows the optical spectrum at the output of MZM with driving sinusoidal RF signal at frequency $f_3 = f_r = 20$ GHz and Fig. 11 shows the optical spectrum at the output of MZM when all the modulators are driven at ($f_1 = f_2 = f_3 = f_r = 20$ GHz). In both cases, it is found that the MZM modulator acts as a subcarrier flatter. Nonlinear effect of IM suppresses the spectral fluctuation and energized the weak sidebands resulting in a flattened spectrum at the output.

Comparison between the above two cases allows us to analyze the feasibility of the proposed OFC generation technique. Based on the theoretical analysis and discussion, it is seen that the main key role is played by the second EAM, which works as subcarrier enhancer when it is driven by a sinusoidal RF signal at frequency $f_r/2$ GHz. However, it provides the negligible change in the number of subcarriers when it is driven at f_r GHz due to the cancellation of spectral components. Here, MZM functions as an IM that performs the amplitude gating of the optical spectrum and energized the weak sidebands to get a flattened spectrum at the output. Therefore, it is found that 63 subcarriers with 10-GHz spacing and within 2-dB power fluctuation are generated through our proposed technique.

4 Conclusion

In this paper, we proposed a technique for the generation of an OFC with good power level and flatness by the cascading of two EAM and one MZM. From the theoretical analysis and simulation results, we conclude that cascaded EAMs generate the ultrashort optical pulses with broadened spectrum in frequency domain but with poor spectral flatness. The spectral flatness can be achieved by further cascading the MZM, which suppresses the spectral fluctuation due to its filtering characteristics and nonlinear effect of IM. Using the proposed OFC generation technique, it is possible to generate 63 subcarriers with 10-GHz spacing and with power variation less than 2 dB. The spectral bandwidth of the generated OFC is 630 GHz. This technique generates ultraflat OFC, which has a great scope in future high-speed optical communication.

References

1. P. J. Delfyett et al., "Optical frequency combs from semiconductor lasers and applications in ultrawideband signal processing and communications," *J. Lightwave Technol.* **24**(7), 2701–2719 (2006).
2. Z. Jiang et al., "Optical arbitrary waveform processing of more than 100 spectral comb lines," *Nat. Photonics* **1**(8), 463–467 (2007).
3. A. R. Criado et al., "Ultra narrow linewidth CW sub-THz generation using GS based OFCG and n-i-pn-i-p superlattice photomixers," *Electron. Lett.* **48**, 1425–1426 (2012).
4. J. Capmany and D. Novak, "Microwave photonics combines two words," *Nat. Photonics* **1**(6), 319–330 (2007).
5. T. Sakamoto et al., "DWDM transmission in O-band over 24 km PCF using optical frequency comb based multicarrier source," *Electron. Lett.* **45**(16), 850–851 (2009).
6. S. Bennett et al., "1.8-THz bandwidth, zero-frequency error, tunable optical comb generator for DWDM applications," *IEEE Photonics Technol. Lett.* **11**(5), 551–553 (1999).
7. A. Akrout et al., "Error-free transmission of 8 WDM channels at 10 Gbit/s using comb generation in a quantum dash -based modelocked laser," in *34th European Conf. Optical Communication*, Brussels, Belgium, Vol. 7, pp. 17–18 (2008).
8. M. Fujiwara et al., "Flattened optical multicarrier generation of 12.5 GHz spaced 256 channels based on sinusoidal amplitude and phase hybrid modulation," *Electron. Lett.* **37**(15), 967–968 (2001).
9. N. Yokota et al., "Harmonic superposition for tailored optical frequency comb generation by a Mach–Zehnder modulator," *Opt. Lett.* **41**(5), 1026–1029 (2016).
10. Y. Dou, H. Zhang, and M. Yao, "Generation of flat optical-frequency comb using cascaded intensity and phase modulators," *IEEE Photonics Technol. Lett.* **24**(9), 727–729 (2012).
11. Y. Dou, H. Zhang, and M. Yao, "Improvement of flatness of optical frequency comb based on nonlinear effect of intensity modulator," *Opt. Lett.* **36**(14), 2749–2751 (2011).
12. D. G. Moodie et al., "Efficient harmonic generation using an electro-absorption modulator," *IEEE Photonics Technol. Lett.* **7**(3), 312–314 (1995).
13. M. Guy, S. Chernikov, and R. Taylor, "Electroabsorption modulators for high speed ultrashort pulse generation and processing," *IEICE Trans. Electron.* **E81-C**(2), 169–174 (1998).
14. C. E. Rogers et al., "Characterization and compensation of the residual chirp in a Mach–Zehnder-type electro-optical intensity modulator," *Opt. Express* **18**(2), 1166–1176 (2010).
15. R. Hui and M. O'sullivan, *Fiber Optic Measurement Techniques*, Academic Press, Amsterdam (2009).
16. H. D. Jung et al., "Nonlinearity suppression of electroabsorption modulator through dual-parallel modulation," *Microwave Opt. Technol. Lett.* **29**(1), 2–5 (2001).

Ujjwal received her BTech degree in electronics and communication engineering from Maharshi Dayanand University, Rohtak. She received her MTech degree in electronics and communication engineering and currently pursuing her PhD in the field of optical communication networks from Indian Institute of Technology (ISM), Dhanbad, India. She has published her research work in several reputed journals and conferences. She is a reviewer for *Optical Engineering*. Her current research interests include resource allocation and network architecture design in optical networks.

Jaisingh Thangaraj is working as an assistant professor at the Department of Electronics Engineering, Indian Institute of Technology (Indian School of Mines), Dhanbad, India. He received his PhD from Indian Institute of Technology Kharagpur, India, in 2017. He has authored/coauthored more than 20 referred journal and conference papers. His current research interests include WDM optical networks, wireless sensor networks, and ad hoc networks.

Downloaded From: https://www.spiedigitallibrary.org/journals/Optical-Engineering on 1/3/2019
Terms of Use: https://www.spiedigitallibrary.org/terms-of-use